Communication

Versatile Sensing Structure: GaP/Au/Graphene/Silicon

Satyendra Kumar Mishra [1],*, Rajneesh Kumar Verma [2] and Akhilesh Kumar Mishra [3]

[1] Electrical Engineering Department, ETS University, Montreal, QC H3C 1K3, Canada
[2] Department of Physics, Central University of Rajasthan, Bandarsindri, Ajmer 305817, India; rkverma@curaj.ac.in
[3] Department of Physics, Indian Institute of Technology, Roorkee 247667, India; akhilesh.mishra@ph.iitr.ac.in
* Correspondence: satyendra-kumar.mishra.1@ulaval.ca

Abstract: A versatile sensing scheme for gas and biomolecule detection has been proposed theoretically using optimized GaP/Au/Graphene/Silicon structures. A Gallium Phosphide (GaP) prism is used as a substrate in the proposed surface plasmon resonance based sensing scheme, which is designed to be in Kretschmann configuration. The thicknesses of different constituent layers have been optimized for the maximum values of the sensitivies of the gas and bio-sensing probes. To delineate the role of the silicon layer, sensing probes without a silicon layer have also been numerically modelled and compared. The present GaP/Au/Graphene/Silicon probes possess higher values of sensitivity for the detection of gas and biomolecules compared to the conventional SPR sensing probes reported in the literature.

Keywords: sensor; graphene; GaP; gold; silicon

1. Introduction

The enticing prospect of concentrating and controlling light at a sub-wavelength scale has inspired tremendous interest in the field of plasmonics [1]. Different waveguide [2] and metamaterial [3,4] geometries have been explored to develop nano antennas [5], optical interconnects [6], super-resolution imaging [7], and different sensing devices [8]. Over the last few decades, steady progress has been made in the development of biosensors in diagnostic, enzyme detection, and food safety, and of gas sensors in industrial safety [1,9,10]. Since its first demonstration by Jorgenson et al., surface plasmon resonance in conjunction with optical fibers has given birth to a new era in the field of sensing [1].

Surface plasmons are the collective oscillation of the free electrons at the metal dielectric interface, leading to the generation of a resonant electric field that decays in a transverse direction exponentially in both of the media [11]. Two configurations have been reported in the literature for the excitation of the surface plasmons—the Kretschmann configuration and the Otto configuration. Out of these two, the Kretschmann configuration is easy to implement. In the Kretschmann configuration, SPR interrogation is performed with either of the following two methods: wavelength interrogation or angular interrogation. In the wavelength interrogation method, the angle of incidence of the exciting light is kept fixed and the wavelength is varied to excite the SPR, while in the angular interrogation method, the wavelength of the exciting light is fixed and the angle of incidence is varied. In the Kretschmann configuration, the metal strip is deposited on the base of the prism and p-polarized light is launch at the metal-prism interface from one of the faces of the prism at an angle greater than the critical angle, and reflected light is detected from the other face. The dielectric medium to be sensed is kept in contact with the metal film at the prism base. The incident light after suffering total internal reflection generates an evanescent wave at the metal dielectric interface, which passes through the metal film and excites the surface plasmons at the metal-dielectric interface, resulting in the transfer of energy to the Surface Plasmon Wave (SPW). We observed that, for a particular incident angle, the reflectivity

of the curve, measured at the other face of the prism, becomes minimum. This angle is known as the resonance angle, and at this particular angle, the propagation constants of the evanescent wave and the surface plasmon wave becomes equal. The resonance angle depends on the refractive index (RI) of the outer dielectric medium, which is kept in contact with the gold layer.

Once the gold layer is activated properly, the phenomenon of surface plasmon resonance can be used for the detection of different gases and biomolecules. When the sample containing biomolecules or gas molecules comes into contact with the metal surface, the biomolecules is adsorbed, whereas the gas molecules reacts with metal film and change the ambient RI, which gets reflected in terms of the shift in SPR (reflection) spectrum. Performance of the sensor depends largely on the absorbance of the gas or biomolecules. Hence, the nature of the gas and biomolecules very much affect the sensor's performance. Recently, graphene has emerged as another material with an important property of high sensitivity towards different gases and bio-molecules. Graphene shows very good mechanical, electrical, and optical properties, which has attracted many researchers and scientists in different areas of research. Graphene, having zero bandgap, high electron mobility, very low resistivity, and a 2D structure, opens a new window into the field of sensing [12].

In the present work, we have carried out a detailed theoretical analysis of a couple of prism-based SPR sensors in the Kretschmann configuration. The prism is made up of GaP material, with a base coated with Au. On top of the Au layer, there is a thin film of graphene, and over that a silicon layer is considered. Silicon has been used to enhance the field and therefore overall sensitivity of the device [13]. GaP is a transparent semiconductor material with a refractive index of approximately 3.3 in the visible range of the spectrum. Additionally, it is a wide band gap material [14]. To excite SPs, the angular interrogation technique is utilized using light in the visible region of 632 nm. In our numerical simulation, the thicknesses of the different layers have been optimized to maximize sensitivity in both the gas and bio-sensing schemes. The study reveals that the proposed configuration for a particular numbers of the graphene layers shows very high sensitivity towards biomaterials, while at other thickness its sensitivity towards gas sensing is high. We have also given a comparative analysis of our results for the GaP/Au/Graphene configuration, i.e., without a silicon layer coated sensor.

2. Basic Theory

If we consider a prism of GaP, the base of the prism is coated with Au film, which is then followed with the graphene and then the silicon layers. The sensing medium (gases and biomolecules) is considered to be in contact with this sensing probe. A schematic diagram of the proposed probe is shown in Figure 1. A somewhat different configuration is studied in [14]. TM-polarized monochromatic light of wavelength 632 nm from a He-Ne laser is made to incident from one face of the prism, and the reflected light is observed from the other face. Because the angular interrogation method is considered, the angle of incidence is varied to achieve phase matching to excite the SPW. At resonance angle, the light is maximally coupled to the surface plasmons, and reflectance shows a corresponding minimum. The position of the reflectance minimum sensitively depends on the sensing medium RI and changes accordingly. For numerical modeling of the proposed probe, the following mathematical relations and parameters are used.

At the given wavelength, the RI of the GaP prism is 3.3 [15] and that of the Silicon is 3.8354 + i 0.0245; i stands for iota [13]. The RI of Gold is calculated from the following dispersion relation [16]:

$$\varepsilon(\lambda) = \varepsilon_r + i\varepsilon_i \ = 1 - \frac{\lambda^2 \lambda_c}{\lambda_p^2 (\lambda_c + i\lambda)}, \tag{1}$$

where $\lambda_p = 168.26$ nm and $\lambda_c = 8934.2$ nm. The dispersion relation of graphene is given as [17].

$$n(\lambda) = 3 + i\frac{C}{3}\lambda, \tag{2}$$

where C is a constant having a value of 0.005446 nm^{-1}, and the wavelength is measured in nm. As graphene is a two-dimensional structure with a sheet thickness of 0.34 nm, its total thickness depends on the total number of layers (L), deposited and calculated as 0.34 * L nm.
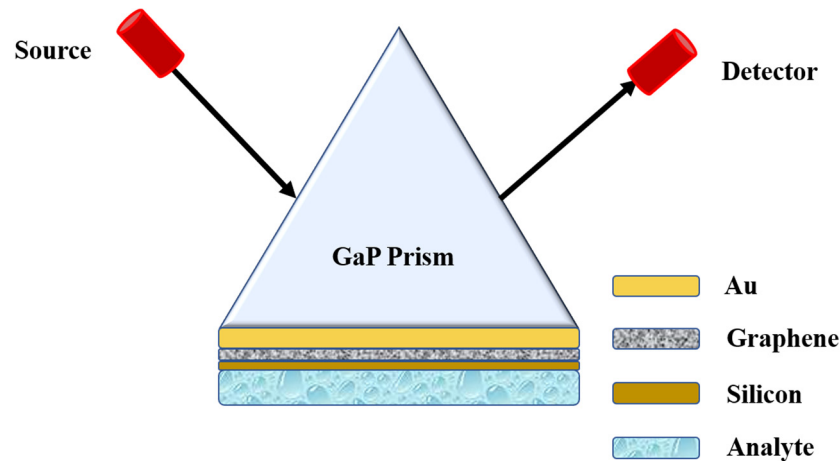

Figure 1. Schematic diagram of the experimental set-up.

For numerical modelling, the N-layer matrix method has been used [18,19]. The characteristic matrix of the N-layer structure can be expressed by:

$$
M = \prod_{k=2}^{N} M_k = \begin{bmatrix} M_{11} & M_{12} \\ M_{21} & M_{22} \end{bmatrix}
= \begin{bmatrix} \cos\beta_k & -i\sin\beta_k/q_k \\ -iq_k\sin\beta_k & \cos\beta_k \end{bmatrix} \tag{3}
$$

where $\beta_k = (2\pi d_k/\lambda)\left(\varepsilon_k - n_1^2\sin^2\theta_1\right)^{1/2}$ and $q_k = \left(\varepsilon_k - n_1^2\sin^2\theta_1\right)^{1/2}/\varepsilon_k$, respectively, where n_k and ε_k are the complex values of the RI and the permittivity of the kth layer with thickness d_k. The reflection coefficient, r_p, of the p-polarized incident wave can be expressed as:

$$r_p = \frac{(M_{11} + M_{12}q_N)q_1 - (M_{21} + M_{22}q_N)}{(M_{11} + M_{12}q_N)q_1 + (M_{21} + M_{22}q_N)} \tag{4}$$

and therefore the reflectance R_p is $R_p = \left|r_p\right|^2$.

In the θ vs.R_p plot, the angle associated with minimum R_p corresponds to resonance angle (θ_{res}).

To evaluate the performance of the sensor, we use sensitivity and detection accuracy (DA) as characterizing parameters, which are defined, respectively, as-

Sensitivity: If, for the change in the RI of the sensing medium by δn_s, the corresponding change in the position of the transmission minima angle is $\delta\theta_{SPR}$, then the sensitivity is defined as [20–22].

$$S_n = \frac{\delta\theta_{SPR}}{\delta n_{res}} \tag{5}$$

The unit of the sensitivity in the angular interrogation method is degree/RIU, while in the wavelength interrogation method it is nm/RIU or μm/RIU. Note that RIU stands for Reftactive Index Unit.

Detection accuracy: DA is defined as the full width at half maximum of the SPR curve [20–22].

3. Results

In this study, we have analyzed the two configurations Au/graphene/silicon and Au/graphene using a GaP prism as a substrate. We have studied gas and biomolecule sensing using the same configurations. For the gas sensing, the RI of the gaseous medium are taken to be 1 RIU and 1.0008 RIU, because most of the gases have an RI close to 1. The position of the dip in the reflectance spectra changes with the adsorption of the gas molecules at the uppermost layer. The optimized thickness of the Au layer in the present configuration is found to be 50 nm [14]. To optimize the design further, sensitivity was calculated for a varying number of graphene layers (L) and for different thicknesses of silicon layer.

In Figure 2, we have plotted the sensitivity versus the number of graphene layers deposited over the Au coated GaP prism. To start with, the silicon layer thickness is taken to be 11 nm. It is observed that, as we increase the number of graphene layers, the sensitivity of the sensor increases up to a particular number of graphene layers and then it saturates for a certain range of graphene thicknesses (L = 13 to 17), and afterwards it decreases. We chose 13 layers of graphene as the optimum number for our design. Note that using thermal evaporation or sputtering coating machines, we can deposit silicon layers at a nm level thickness [19,23]. Normally, a thickness monitor equipment unit is attached to this coating machine, which accurately measures the layer thickness.
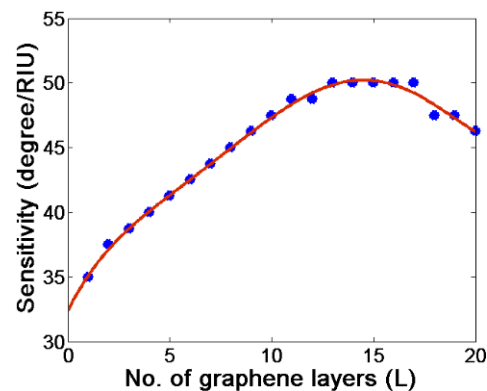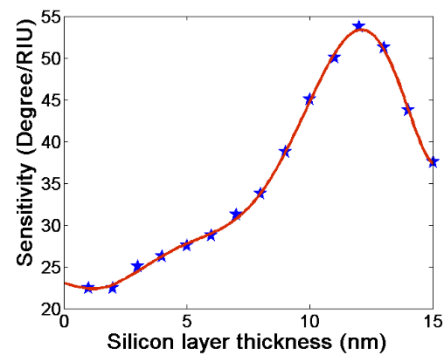

Figure 2. Sensitivity variation with no. of graphene layers for a gas sensing probe with 50 nm of Au and 11 nm of silicon layer thickness. Maximum sensitivity is calculated to be 50 degree/RIU. The circle symbols are simulated data points, which are fitted with red line.

Because graphene is a lossy material, it should decrease the DA of the probe, as observed in Figure 3. The DA is optimal for four layers of graphene. The simulations for DA calculations were performed for an analyte refractive index of 1 RIU.
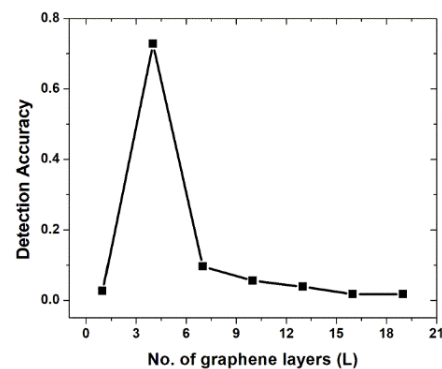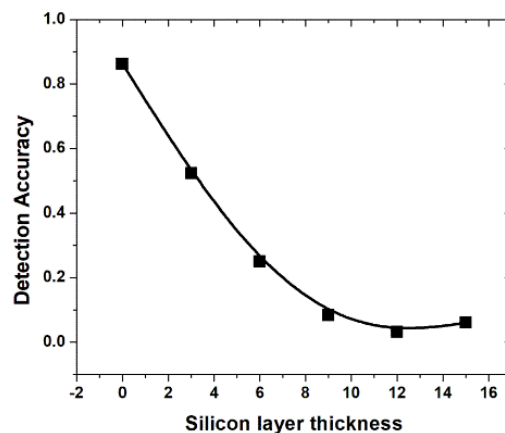

Figure 3. DA variation with no. of graphene layers for gas sensing probe (50 nm of Au, 11 nm silicon) for gaseous medium refractive index 1 RIU. The square symbols are simulated data points, which are fitted with black line.

To optimize the thickness of the silicon layer, we fixed the thickness of the Au layer at 50 nm, used the optimized 13 layers of graphene, and varied the thickness of the silicon to see the sensitivity variation in Figure 4. The maximum sensitivity of 53.75 degree/RIU is observed for a 12 nm thickness of silicon. Thus, the optimized design for gas sensing is Au (50 nm)/graphene (13 layers)/silicon (12 nm), with a sensitivity of 53.75 degree/RIU.

Figure 4. Sensitivity variation with silicon layer thickness for a gas sensing probe with 50 nm of Au and 13 layers of graphene. Maximum sensitivity is calculated to be 53.75 degree/RIU. The star symbols are simulated data points, which are fitted with red line.

We also studied the DA variation in the above design, as shown in Figure 5. Because silicon is a lossy dielectric material, DA decreases with the increasing thickness of the silicon. We would like to note that the simulations were performed for gaseous medium refractive index 1 RIU.

Figure 5. DA with silicon thickness for gas sensing probe graphene layer (L = 13) with 50 nm of Au for gaseous medium refractive index 1 RIU. The square symbols are simulated data points, which are fitted with black line.

To have a comparative study, we have also studied the above sensor without the silicon layer, as shown in Figure 6. The maximum sensitivity for gas sensing in this case is observed to be 33.75 degree/RIU, which is significantly lower than the previously reported value. This establishes the role of the silicon layer as a sensitivity enhancing layer.
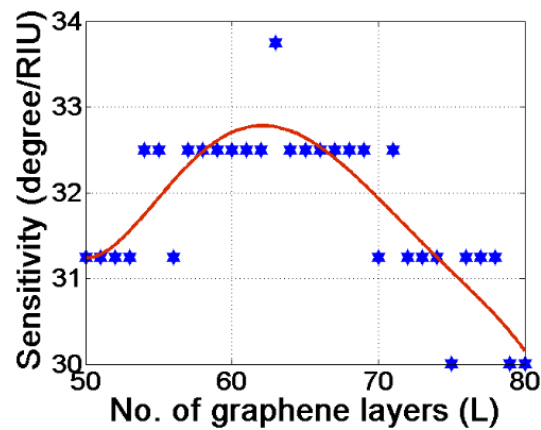
Figure 6. Sensitivity variation with no. of graphene layers for gas sensing probe (without silicon) with 50 nm of Au. Maximum sensitivity is calculated to be 33.75 degree/RIU. The star symbols are simulated data points, which are fitted with red line.

The SPR curve for the optimized gas sensing probe is shown in Figure 7. We have plotted SPR curves for two refractive indices—1 RIU and 1.008 RIU.
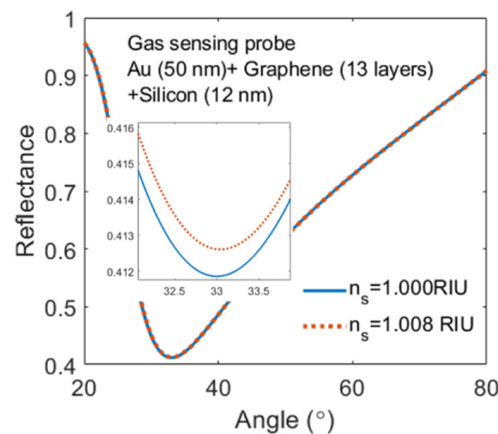

Figure 7. SPR (transmittance) curve for optimized gas-sensing probe with Au (50 nm)/graphene (13 layers)/silicon (12 nm). The inset shows the zoomed-in picture around the SPR dip.

In the following, we have theoretically analyzed the bio sensing performance on the above proposed probe design, but with differently optimized constituent layer thicknesses. For biosensing, we have chosen the RI of the sensing medium, 1.330 RIU, and in the presence of bio-molecules such as bacteria, enzyme, drugs, etc., the sensing medium RI is assumed to shift to 1.335 RIU. To evaluate the sensor performance and to optimize its design, we calculated the sensitivity with 50 nm of Au, varying no. of layers of graphene, and a representative 11 nm thickness of silicon, as depicted in Figure 8. The figure reveals that the maximum sensitivity of the probe towards the bio sample is 66.80 degree/RIU for four layers of the graphene.
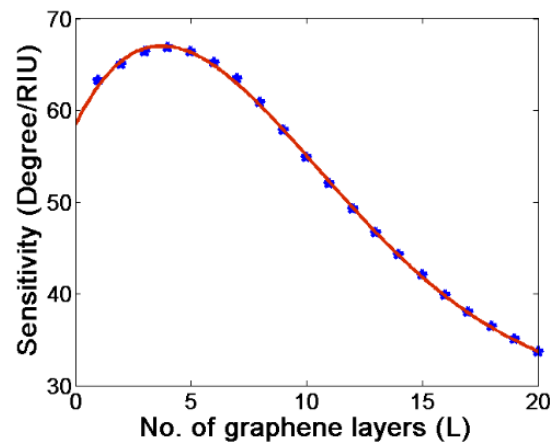
Figure 8. Sensitivity variation with no. of graphene layers for bio sensing probe with 50 nm of Au and representative 11 nm of silicon. Maximum sensitivity is calculated to be 66.80 degree/RIU. The star symbols are simulated data points, which are fitted with red line.

To see the optimized thickness of the silicon layer in the above design, we varied the silicon layer thickness, keeping the Au thickness fixed at 50 nm and no. of graphene layers fixed at four. Figure 9 shows the sensitivity plot for the same and predicts the optimum thickness of the silicon layer to be 12 nm, and the corresponding sensitivity is 72.60 degree/RIU.
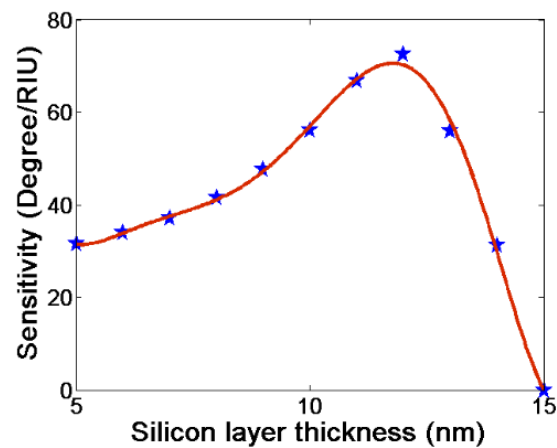
Figure 9. Sensitivity variation with silicon layer thickness for bio sensing probe with 50 nm of Au and four layers of graphene. Maximum sensitivity is calculated to be 72.60 degree/RIU. The star symbols are simulated data points, which are fitted with red line.

Figure 10 shows the corresponding DA plot. We have performed simulation for refractive index 1.33 RIU.
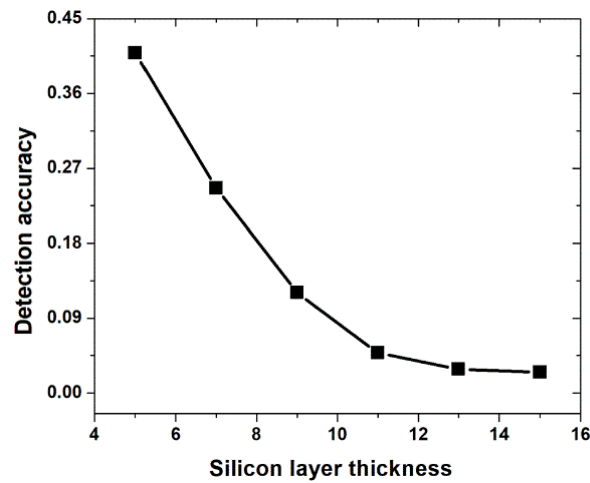
Figure 10. DA with silicon thickness for bio sensing probe graphene layer (L = 4) with 50 nm of Au for refractive index 1.33 RIU. The square symbols are simulated data points, which are fitted with black line.

Figure 11 shows the sensitivity variation for the gas sensing probe with Au 50 nm and varying no. of graphene layers. The silicon layer is absent in this particular case. Maximum sensitivity is calculated to be only 34.40 degree/RIU, which is again very low compared to the probe with a silicon layer. This again confirms the role of silicon in sensitivity enhancement.
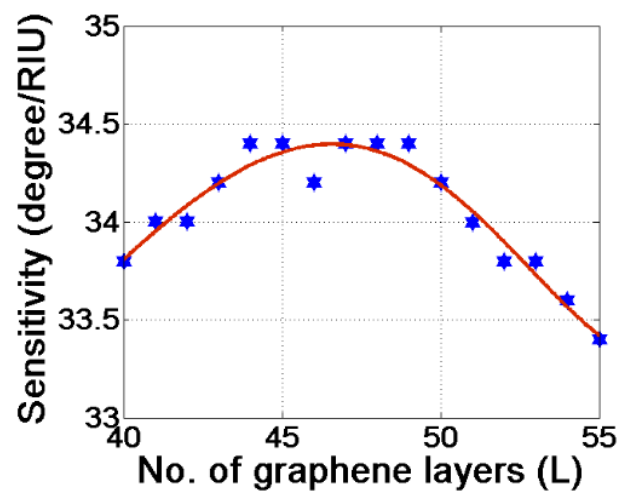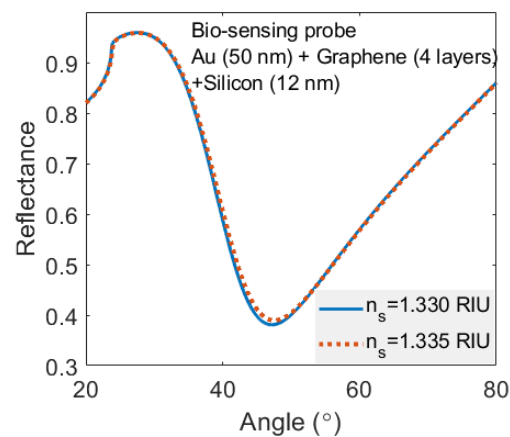

Figure 11. Sensitivity variation with no. of graphene layers for bio sensing probe (without silicon) with 50 nm of Au. Maximum sensitivity is calculated to be 33.75 degree/RIU. The star symbols are simulated data points, which are fitted with red line.

The SPR curve for an optimized bio-probe with Au (50 nm)/graphene (four layers)/silicon (12 nm) is shown in Figure 12.

Figure 12. SPR (transmittance) curve for optimized bio-sensing probe with Au (50 nm)/graphene (four layers)/silicon (12 nm).

4. Conclusions

In summary, a novel SPR-based sensor design, having potential for the detection of both gas and bio samples, has been proposed and characterized. The sensor has a field enhancing silicon layer and an adsorbing graphene layer. The sensitivities for detection of gas and bio samples are calculated to be 53.75 degree/RIU and 72.60 degree/RIU, respectively at an interrogation wavelength of 632 nm. The optimized sensing probe's design parameters for gas and bio-sensing are, respectively, Au (50 nm)/graphene (13 layers)/silicon (11 nm) and Au (50 nm)/graphene (4 layers)/silicon (12 nm). Alongside this, DA analysis has also been performed.

Author Contributions: Conceptualization, S.K.M., R.K.V. and A.K.M.; methodology, S.K.M.; validation, S.K.M., R.K.V. and A.K.M.; formal analysis, S.K.M.; investigation, S.K.M..; data curation, S.K.M.; writing—original draft preparation, S.K.M., R.K.V. and A.K.M.; writing—review and editing, R.K.V. and A.K.M.; visualization, S.K.M.; supervision, A.K.M. All authors have read and agreed to the published version of the manuscript.

Data Availability Statement: Not applicable.

Conflicts of Interest: The authors declare no conflict of interest.

References

1. Jorgenson, R.C.; Yee, S.S. A fiber-optic chemical sensor based on surface plasmon resonance. *Sens. Actuators B Chem.* **1993**, *12*, 213–220. [CrossRef]
2. Rodriguez, S.R.K.; Chen, Y.T.; Steinbusch, T.P.; Verschuuren, M.A.; Koenderink, A.F.; Rivas, J.G. From weak to strong coupling of localized surface plasmons to guided modes in a luminescent slab. *Phys. Rev. B* **2014**, *90*, 235406. [CrossRef]
3. Kumar, A.; Mishra, A.K. Anomalous self-steepening, temporal pulse splitting and ring formation in a left-handed metamaterial with cubic nonlinearity. *J. Opt. Soc. Am. B* **2012**, *29*, 1330–1337. [CrossRef]
4. Chen, X.; Wei, R.R.; Shen, M.; Zhang, Z.F.; Li, C.F. Bistable and negative lateral shifts of the reflected light beam from Kretschmann configuration with nonlinear left-handed metamaterials. *Appl. Phys. B* **2010**, *101*, 283–289. [CrossRef]
5. Yi-Hsun, C.; Min-Hsiung, S.; Kuo-Ping, C. SPR Biosensor Using Gold Nanoantenna Arrays in Kretchmann Configuration. In Proceedings of the Nanotechnology Materials and Devices Conference (NMDC), Tainan, Taiwan, 6–9 October 2013.
6. Pleros, N.; Kriezis, E.E.; Vyrsokinos, K. Optical Interconnects Using Plasmonics and Si-Photonics. *IEEE Photonics J.* **2011**, *3*, 296–301. [CrossRef]
7. Wei, F.; Lu, D.; Shen, H.; Wan, W.; Ponsetto, J.L.; Huang, E.; Liu, Z. Wide Field Super-Resolution Surface Imaging through Plasmonic Structured Illumination Microscopy. *Nano Lett.* **2014**, *14*, 4634–4639. [CrossRef]
8. Mishra, A.K.; Mishra, S.K.; Gupta, B.D. SPR based fiber optic sensor for refractive index sensing with enhanced detection accuracy and figure of merit in visible region. *Opt. Commun.* **2015**, *344*, 86–91. [CrossRef]
9. Chandra, P.; Noh, H.-B.; Shim, Y.-B. Cancer cell detection based on the interaction between an anticancer drug and cell membrane components. *Chem. Commun.* **2013**, *49*, 1900–1902. [CrossRef]

10. Mishra, A.K.; Mishra, S.K.; Gupta, B.D. Gas-Clad Two-Way Fiber Optic SPR Sensor: A Novel Approach for Refractive Index Sensing. *Plasmonics* **2015**, *10*, 1071–1076. [CrossRef]

11. Homola, J. Surface Plasmon Resonance Based Sensors. *Springer Ser. Chem. Sens. Biosens.* **2006**, *4*, 1452.

12. Kuila, T.; Bose, S.; Khanra, P.; Mishra, A.K.; Kim, N.H.; Lee, J.H. Recent advances in graphene-based biosensors. *Biosens. Bioelectron.* **2011**, *26*, 4637–4648. [CrossRef]

13. Shalabney, A.; Abdulhalim, I. Electromagnetic fields distribution in multilayer thin film structures and the origin of sensitivity enhancement in surface plasmon resonance sensors. *Sens. Actuators A Phys.* **2010**, *159*, 24–32. [CrossRef]

14. Verma, R.K.; Gupta, B.D.; Jha, R. Sensitivity enhancement of a surface plasmon resonance based biomolecules sensor using graphene and silicon layers. *Sens. Actuators B Chem.* **2011**, *160*, 623–631. [CrossRef]

15. Motogaito, A.; Nakamura, S.; Miyazaki, J.; Miyake, H.; Hiramatsu, K. Using surface-plasmon polariton at the GaP-Au interface in order to detect chemical species in high-refractive-index media. *Opt. Commun.* **2015**, *341*, 64–68. [CrossRef]

16. Verma, R.K.; Gupta, B.D. Surface plasmon resonance based fiber optic sensor for the IR region using a conducting metal oxide film. *J. Opt. Soc. Am. A* **2010**, *27*, 846–851. [CrossRef]

17. Bruna, M.; Borini, S. Optical constants of graphene layers in the visible range. *Appl. Phys. Lett.* **2009**, *94*, 031901. [CrossRef]

18. Hansen, W.N. Electric Fields Produced by the Propagation of Plane Coherent Electromagnetic Radiation in a Stratified Medium. *J. Opt. Soc. Am.* **1968**, *58*, 380–388. [CrossRef]

19. Mishra, A.K.; Mishra, S.K. MgF_2 prism/Rhodium/Graphene: Efficient refractive index sensing structure in optical domain. *J. Phys. Condens. Matter* **2017**, *29*, 145001. [CrossRef]

20. Mishra, S.K.; Mishra, A.K. ITO/Polymer matrix assisted surface plasmon resonance based fiber optic sensor. *Results Opt.* **2021**, *5*, 100173. [CrossRef]

21. Mishra, S.K.; Tripathi, D.C.; Mishra, A.K. Metallic grating-assisted fiber optic SPR sensor with extreme sensitivity in IR region. *Plasmonics* **2021**, *11*, 11468. [CrossRef]

22. Mishra, S.K.; Malviya, K.D.; Mishra, A.K. Highly sensitive plasmonic bimetallic sensing probe for aqueous samples. *Opt. Quantum Electron.* **2020**, *52*, 284. [CrossRef]

23. Singh, S.; Mishra, S.K.; Gupta, B.D. Sensitivity enhancement of a surface plasmon resonance based fibre optic refractive index sensor utilizing an additional layer of oxides. *Sens. Actuators A* **2013**, *193*, 36–140. [CrossRef]